Structure and chemical durability of lead crystal glass

Frederic Angeli, Patrick Jollivet, Thibault Charpentier, Maxime Fournier, S. Gin

STRUCTURE AND CHEMICAL DURABILITY OF LEAD CRYSTAL GLASS

Frédéric ANGELI[a], Patrick JOLLIVET[a], Thibault CHARPENTIER[b], Maxime FOURNIER[a], Stéphane GIN[a]

[a]*CEA, DEN, DTCD, SECM, F-30207 Bagnols-sur-Cèze, France*

[b]*NIMBE, CEA, CNRS, Université Paris-Saclay CEA Saclay 91191 Gif-sur-Yvette, France*

ABSTRACT

Silicate glasses containing lead, also called lead crystal glasses, are commonly used as food product containers, in particular for alcoholic beverages. Lead's health hazards require major attention, which can first be investigated through the understanding of Pb release mechanisms in solution. The behavior of a commercial glass containing 10 mol% of PbO (28 wt%) was studied in a reference solution of 4% acetic acid at 22, 40 and 70°C at ea rly and advanced stages of reaction. For the first time, high-resolution ^{17}O solid-state NMR was used to probe Pb in the pristine and altered crystal glass. Inserted into the vitreous structure between the network formers as Si-O-Pb bonds, Pb does not form Pb-O-Pb clusters which are expected to be more easily leached. A part of K is located near Pb, forming Si-O-(Pb,K) mixing areas near the non-bridging oxygens. Pb is always released into the solution following a diffusion controlled process over various periods of time, at a rate between one and two orders of magnitude lower than the alkalis (K and Na). The preferential release of alkalis is followed by an *in situ* repolymerization of the silicate network. Pb is only depleted in the outermost part of the alteration layer. In the remaining part, it stays mainly surrounded by Si in a stable structural configuration similar to that of the pristine glass.

INTRODUCTION

For thousands of years, lead has been used in the preparation of silicate glasses, in particular because it enables the temperature range of the glass-forming ability to be extended. It was widely used in various archeological artifacts, such as enamels and glazes [1], but also in applications for optics, electronics [2] or even in protection against irradiation [3]. Since the 17th century, lead oxide has been added to alkali silicate to form a material called lead crystal, giving a high clarity and a characteristic sonority. Lead crystal has been regulated since 1969 in order to guarantee the quality of the material, based on density, refraction index and lead content criteria. Lead oxide must be at least 24 wt% to be designated as crystal.

Exposure to Pb is hazardous for the environment and for human health when it accumulates in the organism [4, 5]. It is therefore of primary importance to understand the behavior of this element in manufactured articles throughout their conditions of use, particularly if they contain liquids intended for human consumption.

Numerous empirical studies have been carried out to examine the Pb leaching from glass or from glass ceramic in reactive environments, particularly in contact with different actual beverages or simple synthetic solutions such as acetic acid or nitric acid [6-20]. In commercial lead crystal glasses, it has generally been observed that the release of alkalis and Pb ions exhibited a square root time dependence through a diffusion process [11, 15, 17, 18]. Their leaching kinetics usually increase with the temperature and with the acetic acid concentration [17]. During successive contacts, a decrease in the release of Pb has been observed with each additional solution contact [16]. However, there is a lack of mechanistic understanding able to account for and predict the Pb behavior, in relation with its structural evolution during leaching.

The structural arrangements coming from the incorporation of Pb into an alkali silicate network can significantly modify glass macroscopic properties, in particular its chemical durability [10]. For a low content, typically under 40 mol% of PbO, a major part of Pb may be assimilated to a modifier cation [21], thus resembling an alkaline-earth type cation, forming ionic bonds with non-bridging oxygens (NBOs) [22]. When a large amount of Pb is added to reach an orthosilicate composition (Pb/Si = 2), oxygens are then linked to the metallic cations to form metal-bridging oxygen bonds Pb-O-Pb [23]. Pb is then associated in trigonal pyramids connected by their edges to form interlinked Pb_2O_4 units [24]. In this case, Pb mainly takes a network former configuration, forming more covalent bonds with the oxygens [21, 25, 26]. For contents greater than ~60 mol% of PbO, Pb forms its own vitreous network [27]. Pb has the special feature of having ability to form a glass in a very wide range of concentration [28], up to more than 80 mol% of PbO for a rapidly-quenched glass [23, 27]. When Pb acts as a network former cation,

unlike most network formers, it does not provide to the glass a greater chemical durability: Pb clusters form extended lead-rich domains which are rapidly leached. There are percolation pathways between these domains, and the Pb release into solution strongly increases [10]. Generally, whatever the solution pH, the release of Pb seems to decrease when its content is lower [10, 19, 29].

The mechanisms of aqueous alteration of lead crystal glasses compared to their structural evolution during leaching had not been approached prior to this study. In order to give new insights into the understanding of Pb leaching of industrial glasses, a structural approach for the glass as well as its alteration layer is applied, together with the evolution of the elemental alteration profiles. Combined with the solution analyses under various experimental conditions, it enables the mechanisms involved to be better defined.

This work is focused on a commercial lead crystal glass containing 10 mol% of PbO (28 wt%). Complementary experiments, which enabled various kinetics regimes to be reached, are conducted to simulate the short and long term behavior of the crystal glass. Hydrolysis mechanisms were investigated using dynamic experiments with high flow rate whereas interdiffusion mechanisms were highlighted from static experiments using saturated solutions with respect to amorphous silica (ion-exchange processes are not affected by solution saturation). The experiments were carried out in 4% (*v/v*) acetic acid solution, which is commonly used as a standard reference solution [13, 17, 30]. The local structure of pristine and altered materials was characterized by high-resolution solid-state Nuclear Magnetic Resonance (NMR) of silicon-29 and oxygen-17. Elemental depth profiling were monitored by Time-of-Flight Secondary Ion Mass Spectrometry (ToF-SIMS).

EXPERIMENTAL

Materials.

Two glasses were used for this study, the first being a commercial glass with the molar composition $77.1SiO_2 – 0.8Na_2O – 11.3K_2O – 10.6PbO – 0.2Sb_2O_3$. A second glass was synthetized to be enriched in oxygen-17 (without Sb addition). 200 mg of glass was prepared by sol-gel from a mixture of alkoxides hydrolyzed by 90% enriched water in ^{17}O [31]. After reaction, this mixture was maintained at 1270 ℃ for 30 minutes under argon atmosphere in a Pt/Au crucible. ICP-OES analysis after acidic dissolution ($HCl+HNO_3+HF$) gave the molar composition: $80.7SiO_2 – 0.7Na_2O – 10.8K_2O – 7.9PbO$.

NMR.

^{29}Si MAS NMR data were collected on a Bruker 300WB Avance I spectrometer operating at a magnetic field of 7.02 T. (I = 1/2, Larmor frequency ν_0 = 59.4 MHz). A Bruker 4 mm (outer diameter of the rotor) CPMAS Probe was used at a spinning frequency of 10 kHz. Silicon spectra were acquired

using the CPMG sequence [32], by typically accumulating 32 echoes with an echo delay of 4 ms between consecutive 180° pulses. The echoes were then summed up and Fourier transformed to obtain the spectra. A 20 s recycling time was used; checks were carried out that no spectral deformation was observed for longer recycling delays (up to 1200 s). The spectra were referenced to an external tetrakis(trimethylsilyl)silane (TKS) sample, for which the highest intensity peak was situated at −9.9 ppm from that of TMS.

^{17}O MAS NMR data were collected on a Bruker 500WB Avance II spectrometer operating at a magnetic field of 11.72 T (I = 5/2, Larmor frequency ν_0 = 67.67 MHz,). A Bruker 4 mm CPMAS probe was used at a spinning frequency of 12.5 kHz. MAS NMR spectra were acquired using a rotor synchronized Hahn echo pulse sequence to minimize the baseline distortion, with soft 90° and 180° pulses (selective on the central transition, RF field 25 kHz), an echo delay of one rotation period and a recycle delay of 1 s (no change in lineshape was observed for longer delay). The MQMAS spectra were acquired with 64 t_1 rotor-synchronized increments (of one rotation period) in the first dimension and a 1 s repetition time (4500 FIDs per t_1 value were collected). The Z-filter pulse sequence [33] was used with first and second pulse durations of 5 µs and 2 µs, respectively (RF field 60 kHz), and a third 90° soft pulse, selective on the central transition , of 3.5 µs (RF field 25 kHz) [34].

All data were processed and fitted using an in-house written software [35].

ToF-SIMS.

Depth profiles were analyzed by ToF-SIMS IONTOF® TOF 5 using O_2^+ sputtering beams analyzing a surface area of 60 x 60 µm^2. Oxygen beam was tuned at 2 kV, 500 nA. Elemental profiles were normalized to that of Si to avoid matrix effects.

Leaching experiments.

After crushing and sieving, the selected size fractions (20-40 and 63-125 µm) were washed by decantation in acetone and absolute ethanol to remove fine particles, according to Stokes' law. Then the specific surface areas of the glass powders were measured by krypton physical adsorption on the sample surface with the BET method on a Micromeritics ASAP 2020.

Forward dissolution rate r_0 was measured using a single-pass flow-through test (SPFT) at 22, 40 and 70 °C. About 100 mg of glass powder (63-125 µm particle size fraction) were placed into a column made of PTFE tube, through which 4% (*v/v*) acetic acid was passed at a flow rate between 0.2 and 0.6 mL/min to avoid any feedback effect on the rate by glass constituent elements released into solution. The temperature of the leaching solution was monitored continuously at the reactor inlet and a maximum variation of ± 1 °C was allowed. The leachate was regularly sampled and the Si concentration was determined photometrically with a Merck Spectroquant test and a Cary Varian UV-

visible spectrophotometer with a method analogous to ASTM D859-10. Taking into account the errors on the glass surface area and the Si concentration, the uncertainty on r_0 was about 10%. The normalized mass losses, NL_i, (g.m^{-2}) were calculated with the equation (1):

$$NL_i(t) = \sum_{j=1}^{j=n} \frac{1}{x_i \times SSA \times m} \left[\frac{(C(i)_j + C(i)_{j+1})}{2} \times Q \times (t_{j+1} - t_j) \right] \quad (1)$$

with j the sampling, $C(i)_j$ the concentration of the element in the j^{th} sampling, Q the solution flow rate, SSA the specific surface area of powder sample, m the mass of glass, x_i the weight fraction of element i in the glass, and $t_{j+1} - t_j$ the time between two samplings.

Alteration in static conditions was measured in perfluoroalkoxy reactors (PFA) at 22, 40 and 70 ℃ in 4% (*v/v*) acetic acid solution. The mass of glass powder (20-40 µm and 63-125 µm particle size fractions) was adjusted to have the desired glass-surface-area-to-solution-volume ratios (*SA*/V). The solutions were ultrafiltered (cutoff 10 kDa) and analyzed by ICP-OES.

$$NL(i)_t = NL(i)_{t-1} + \frac{(C(i)_t - C(i)_{t-1}) \times V_t}{SSA \times m \times x_i} \quad (2)$$

with $C(i)_t$ the concentration of the element i in solution at time t, and V_t the volume of solution sampling at time t.

The equivalent thickness of altered glass is given by:

$$ETh(i) = \frac{NL(i)}{\rho} \quad (3)$$

ρ is the glass density (3.028.10^6 kg.m^{-3}). The uncertainties for $ETh(i)$ and the alteration rate $r = dETh(i)/dt$ are of 10% and 30%, respectively.

RESULTS AND DISCUSSION

Glass structure

^{29}Si MAS NMR.

Two contributions were observed at −94 ppm and −106 ppm on the ^{29}Si MAS NMR spectra for pristine glass (Figure 1a), which correspond respectively to the Q^3 and Q^4 entities, in agreement with the data obtained on lead silica binary glasses [36, 37]. The simulation of the ^{29}Si spectra gave a proportion of 59% of Q^3 and 41% of Q^4 units (see supplementary information, Figure S1). The

resulting number of NBOs is then 25.7%. The calculation of the NBOs based on the glass composition, considering that two NBOs are formed from Na_2O, K_2O and PbO (without postulating free oxygen atoms) leads to a value of 25.6%, very close to the experimental value.

^{17}O MAS NMR.

The ^{17}O MAS spectrum of the pristine glass (Figure 1b) enables three contributions to be resolved. A wide line at the −20 to 50 ppm range with a characteristic second-order quadrupolar lineshape corresponds to the bridging oxygens Si-O-Si. Two narrower featureless peaks centered on 70 and 110 ppm are related to the NBOs and may be attributed to Si-O-K and Si-O-(Pb,K), respectively (the latter corresponds to regions where Pb and K are mixed together but without forming Pb-O-Pb bonds). This attribution will be discussed hereafter from the MQMAS data.

^{17}O MQMAS NMR.

The three contributions related to Si, K and Pb are clearly separated on the experimental and simulated ^{17}O MQMAS spectra shown in Figure 2a. The simulated spectra, generated using a 3D distribution of the NMR parameters (taking into account the correlation effects between these parameters [35]), show very good agreement with the experimental spectra (Figure 2a). Figure 2b shows the two-dimensional projection of the distribution of the NMR parameters, the isotropic chemical shift (δ_{iso}) and the quadrupolar coupling constant (C_Q) extracted from the MQMAS spectra. Lee and Kim [38] recently reported the structural evolution of binary lead silicate glasses from ^{17}O MQMAS NMR for high PbO contents close to the orthosilicate composition ranging from 60 mol% to 71 mol%. They clearly pointed out the presence Pb-O-Pb bonds which increased with Pb content at the expense of Si-O-Si bonds. They represented Pb and Si mixing sites in the form $^{[n]}$Pb-$^{[m]}$O-$^{[4]}$Si, where n = 3,4 and m = 2,3,4. Under these conditions, the same oxygen atom could be involved in both Pb-O-Si and Pb-O-Pb bonds. The absence of Pb-O-Pb contribution (within the NMR detection limit) in our crystal glass suggests that Pb structural configuration may be fairly close to that of an alkaline-earth type network modifier.

Furthermore, the nature of the alkali cation at the origin of the NBO formation may modify the position of the ^{17}O line; a sodium disilicate decreases the NBO δ_{iso} by about 40 ppm compared to a potassium disilicate [39]. The position of the NBO site at around 75 ppm can be attributed here to Si-O-K, Si-O-Na being expected at around 40 ppm [35]. Given the low Na content in the glass (below one percent) and the sensitivity of the MQMAS experiment, it remains challenging to observe Si-O-Na contribution on the ^{17}O MQMAS spectra.

A previous work carried out on a binary sodium silicate glass with a 77 mol% SiO_2 content close to that studied here reported ^{17}O NMR parameters for the Si-O-Si site similar to those obtained

for our lead glass [35]. Under these conditions, the addition of Pb to the glass does not seem to have a major effect on the Si-O-Si site geometry, either for the angular distributions (which influence the quadrupolar parameters [40-42]) or the Si-O bond distances (which influence the isotropic chemical shift [43, 44]). In the binary lead silicate glasses studied by Lee and Kim [38], the Si-O-Pb δ_{iso} was located around 151 ppm and it slightly increased with Pb content. For our glass composition, the contribution related to Pb is close to 119 ppm (see Table 1). The quantification of the three oxygen contributions enables the origin of this difference to be discussed.

By first assuming that the three ^{17}O sites revealed by the NMR spectra can be attributed to the contributions of Si-O-Si, Si-O-Pb and Si-O-K, Table 1 compares their proportions calculated from the crystal glass chemical composition and those obtained from the NMR data. It clearly appears that the quantity of Si-O-Pb (14%) is considerably greater than expected from the composition (8.7%), unlike for Si-O-K where the quantity is lower (8% experimentally instead of the expected 12.7%). This observation indicates that Si-O-Pb contribution does not only contain Pb and Si cations, but rather a mixing of Pb and K, noted Si-O-(Pb,K), as had been previously observed for other types of cations having fairly close ionic radii [45, 46]. Under these conditions, Si-O-(Pb,K) site would consist of 38% of K and 62% of Pb. This effect thus explains the lower ^{17}O δ_{iso} of the Si-O-Pb site in the glasses studied here compared to the binary glasses [38]; Si-O-(Pb,K) site at 119 ppm is situated between Si-O-K at 75 ppm and Si-O-Pb at 151 ppm. Finally, it should be noted that the wider distribution of ^{17}O δ_{iso} for Si-O-(Pb,K) is probably the result of a greater structural and/or chemical disorder for this mixing site.

It is worth noting that by taking into account the difference in chemical shift between Si-O-Pb at 151 ppm and Si-O-K at 75 ppm, weighting of the value obtained for Si-O-(Pb,K) at 119 ppm would give a K quantity of 42%, very close to the value directly deduced from the quantification of the MQMAS spectrum (38%). It would therefore appear that ^{17}O δ_{iso} of Si-O-(Pb,K) could provide information regarding the proportion of K mixing with Pb in the NBO environment.

GLASS LEACHING.

For the first set of experiments, the most favorable conditions for accessing silicate network hydrolysis mechanisms were chosen, based on a high renewal rate of a 4% (*v*/*v*) acetic acid solution. Figures 3(a,b,c) show the equivalent alteration thicknesses of Na, K, Pb and Si at 22, 40 and 70 °C calculated from their normalized mass losses (Eq. (3)). The leaching of Sb (not shown) is very close to the Si. An activation energy for hydrolysis mechanisms in the forward dissolution rate regime, based on an Arrhenius law, is given from the Si release (Figure 3d). The linearity between the three temperatures shows the good agreement of the data, resulting in an activation energy of 38.7 ± 1.7 kJ.mol^{-1}. Within the temperature range studied (22-70°C), the release of Si leading to the hydrolysis of the silicate network would thus seem to be controlled by the same mechanisms. It should be noted

that the dissolution was significantly non-congruent; while the release of Pb and Sb were fairly close to the Si network former, K and Na were released much more rapidly. It is tricky to calculate unique activation energy for Pb, K and Na as the non-linearity observed between the three temperatures strongly suggest that the leaching of these elements could not only resulted from network hydrolysis but also interdiffusion. At low temperature, the interdiffusion mechanism may probably favored whereas at higher temperature hydrolysis may be prevalent.

For the second set of experiments, a solution initially saturated with respect to amorphous silica [47] was used in order to specifically focus on the interdiffusion mechanisms. It has recently been showed that there was no hydrolysis of Si under these conditions [47]. Figure 4(a,b,c) compares the normalized mass losses for K and Pb at 22, 40 and 70 ℃ as a function of the square root of time. The very low concentration of Na in the glass (0.2 mol%) made its measuring in solution only possible at 70℃. It was then observed that it behaved like K. Analogous behavior of Na and K is therefore probable at lower temperatures.

The resulting linear behavior suggests that the different cations are released in solution by a diffusive mechanism. The leaching of Pb was much lower than K. The Pb behavior thus seems to be assimilated with multivalent elements, like the alkaline earths or the rare earth elements, which are leached much more slowly than the alkalis [46]. Fick's second law was used to derive the apparent diffusion coefficients at the interface between the glass and the solution by fitting the curves in Figures 4(a,b,c). The concentration in solution is then given by [48]:

$$C(i) = 2\frac{SSA \times m}{V} x_i \left(\frac{D_i \times t}{\pi}\right)^{\frac{1}{2}} \quad (4)$$

where $C(i)$ is the concentration of element i (i = K or Pb) in solution, x_i is the concentration of Pb or K in the glass, V the volume of the solution and D_i the diffusion coefficient for Pb or K.

Figure 4d shows the evolution of the diffusion coefficients as a function of the temperature for Pb and K. The resulting activation energies highlight a temperature dependence which is much lower for Pb than for K, with values of 37.2 ± 6.5 kJ.mol^{-1} and 72.2 ± 7.6 KJ.mol^{-1}, respectively. At 22 ℃, a low diffusion coefficient of (3.1±0.6).10^{-22} m^2.s^{-1} is determined for Pb. Depending on the temperature, Pb release into solution is between one and two orders of magnitude slower than the alkalis.

For higher Pb contents, from 25 to 70 mol%, diffusion coefficients of more than four orders of magnitude higher were obtained in glasses altered in 0.1 N or 0.5 N HNO_3 solutions [8, 10]. A percolation mechanism through the plumbate sub-network was observed. Binary lead silicate glasses with PbO starting from an approximately 33 mol% content, had a diffusion coefficient increasing by about one order of magnitude when PbO content increased by 5% [10]. One single composition was studied at a

lower Pb content (25%) below the percolation threshold; it showed less pronounced diffusion coefficient variations, of about 10^{-17} $m^2.s^{-1}$ suggesting a plateau. If this latter value is not taken into account, so if the data located within the percolation regime are extrapolated from our glass composition containing 10 mol% of PbO, a similar value (10^{-22} $m^2.s^{-1}$) compared to that found in our study (10^{-21} $m^2.s^{-1}$) is obtained. This value is far away from the plateau which was observed at approximately 10^{-17} $m^2.s^{-1}$ for 25 mol% of PbO (see supplementary information, Figure S2). Then, the sharp drop in the diffusion coefficient could be due to a second percolation threshold, which would explain the high difference between 10 and 25 mol% of PbO. The formation of Pb-O-Pb bonds with the increase in the Pb concentration, even if they do not yet constituted a plumbate sub-network, could lead to this first percolation threshold beyond which an increase in Pb release kinetics would occur.

Finally, in order to reach more advanced reaction progress, a third set of experiments were carried out in static conditions at different *SA/V* ratios, varying from 10 m^{-1} to 10000 m^{-1}. These long term experiments were conducted at 22 °C in 4% acetic acid solution, without Si in the initial solution, for one year of leaching. Although there were four orders of magnitude between the surface ratios, Figure 5 reports small variations in the leaching of Pb and K, showing that their releases remain controlled by interdiffusion at 22 °C. As expected from our previous experiments, Pb leaching is much lower than K. The calculation of the retention factor for Pb compared to K ($RF_{r(Pb)}$=1−*ETh*(Pb)/*ETh*(K)) gave similar values, with an average retention of 77% of Pb in the alteration layer. It may be noted that Pb concentrations in solution always remain much lower (by at least three orders of magnitude) than the solubility of lead acetate [49]. This confirms that the release of Pb is not controlled by its solubility limit, but rather by diffusion mechanisms.

ALTERATION LAYER CHARACTERIZATION

ToF-SIMS.

Figure 6 displays the elemental profiles obtained by ToF-SIMS on the glass altered at 70 °C in an acetic acid solution saturated with respect to amorphous silica after 1, 7 and 53 days. The progress of the alteration front on the glass surface is clearly visible over time. At the interface between the pristine glass and the alteration layer, the hydration front can be seen progressing, with a greater penetration of hydrogen compared to the alkalis depletion. The profiles for Na and K are very similar, in agreement with the concentrations measured in solution (Figure 4c). Pb was clearly released to a lesser extent than the alkalis, and is only depleted on a thin external surface of the alteration layer. After 53 days, the depth of Pb depletion was fifteen times less than the total thickness of the alteration layer. The equivalent thicknesses for the different elements are in quite good agreement with the depths obtained from the ToF-SIMS profiles. The small differences which remained between the two methods could be explained because (i) calculation of *ETh* using the *SSA* of glass powder measured

by BET underestimates *ETh* [50] (ii) a part of K (~20-30%) is retained in the alteration layer and therefore not released in solution and (iii) it may exist variations in the abrasion rate of ToF-SIMS between the alteration layer external surface and the pristine glass, because of potentially different densities.

The elemental profiles obtained after one year of alteration at various SA/V ratios at 22 ℃ were very similar than the profiles obtained at 70 ℃ for shorter periods. In particular, the three ar eas remain still observed: the hydration front, the alkalis depletion and the Pb-depleted external surface which is still maintained for long term experiments (see supplementary information, Figure S3).

MAS NMR.

Small glass powders of a few microns were entirely altered under static conditions at 70℃ in a 4% acetic acid solution containing oxygen-17 enriched water, in order to specifically probe the alteration layer by ^{17}O NMR. An experiment in oxygen-16 carried out in parallel and under the same *SA/V* ratio conditions (but with a greater volume of solution), enabled the concentrations of elements in solution to be measured. This allowed the experiment to be stopped when all the glass had been altered, based on the release of Na in solution, and to estimate the alteration layer molar composition deduced from the solution analysis: $88.7SiO_2$– $2.5K_2O$ – $7.9PbO$ – $1.0Sb_2O_3$.

Figure 1a compares the ^{29}Si MAS spectra for pristine glass and for glass altered in oxygen-17. An obvious reorganization within the alteration layer through a silicate network polymerization is clearly highlighted. Centered on the Q^2-Q^3 species in the pristine glass, a majority of the Si forms Q^4 units in the alteration layer. Quantification of the NBOs was carried out based on the ^{17}O NMR data of Figure 1b (reported in Table 1). The ^{17}O MAS spectrum clearly confirms that most of K had been released in solution whereas a significant part of Pb remained in the alteration layer. The line corresponding to the Si-O-(Pb,K) contribution, shifted towards the higher chemical shifts, becomes closer to the Si-O-Pb contribution observed in binary lead silicate glasses [38], indicating a lower level of mixing between Pb and K. This shows that in the Si-O-(Pb,K) site, K is preferentially extracted compared to Pb.

Simulation of the ^{17}O MAS spectrum for altered glass was used to estimate the composition of the alteration layer from the various contributions. The following molar proportions were obtained: $93SiO_2$ − $1K_2O$ − $6PbO$ (there was no Sb in this glass), in quite good agreement with the mass balance found from the solution analysis ($88.7SiO_2$ − $2.5K_2O$ − $7.9PbO$ – $1.0Sb_2O_3$). It should however be noted that the NMR indicates a higher SiO_2 content (93% instead of 89%). This is related to the presence of Si-OH sites which overlay the Si-O-Si contribution on the spectrum [51]. These sites were revealed from 2D heteronuclear correlations maps ($^1H \rightarrow ^{17}O$ HETCOR) (see supplementary information, Figure S4a). The NMR parameters considered for this site (Table 1) come from the work

of Brunet et al. [51]. Simulation of the ^{17}O MAS spectrum gave 4% of Si-OH sites (see supplementary information, Figure S4b). The total number of NBOs of 11% is quite comparable to the number of NBOs deduced from the alteration layer composition (10.9%). The repolymerization led to a decrease in the NBOs, dropping from 22% in the glass to 11% in the alteration layer (Table 1). A significant decrease can be noted for the widths of the NMR parameters distribution for the Si-O-Si site (related to higher Si-O-Si mean bond angles), as well as an increase in the quadrupolar coupling constant, closer to that in vitreous silicon [52]. These findings highlight the reorganization of the polymerized silicate network (Q^4).

The behavior of Pb is closely related to the structural configuration it adopts, as much in the pristine glass as in the alteration layer. Homogeneously dispersed within the silicate network, the leaching of Pb is less favorable, and its release into solution is lower than the alkalis. When present at higher concentration than in the glass studied here, Pb may form clusters, and its leaching increases, probably as soon as it forms Pb-O-Pb bonds. For 45 wt% of PbO in a glass containing Na and K, it has been reported that the alkalis and the lead were released at the same rate [11]. At higher concentration, there is a percolation of the Pb sub-network, which is preferentially highly released into solution. These high Pb contents seem to give rise to a surface enrichment in Pb [11, 12]. No such enrichment was observed for our 28 wt% PbO glass; conversely, Pb is depleted in the outermost part of the alteration layer. In the remaining part, it stays surrounded by Si in a stable structural configuration similar to that of the pristine glass.

The data obtained from this work could enable parameters to be set for a simple predictive mechanistic model for lead leaching from commercial lead crystal glass.

REFERENCES

1. Szaloki, I.; Braun, M.; Van Grieken, R., Quantitative characterisation of the leaching of lead and other elements from glazed surfaces of historical ceramics. *J. Anal. At. Spectrom.* **2000,** *15*, (7), 843-850.
2. Cohen, B. M.; Uhlmann, D. R.; Shaw, R. R., Optical and electrical properties of lead silicate glasses. *Journal of Non-Crystalline Solids* **1973,** *12*, (2), 177-188.
3. Barker, R. S.; McConkey, E. A.; Richards.Da, EFFECT OF GAMMA RADIATION ON OPTICAL ABSORPTION OF LEAD SILICATE GLASS. *Phys. Chem. Glasses* **1965,** *6*, (1), 24-&.
4. Patrick, L., Lead toxicity, a review of the literature. Part 1: Exposure, evaluation, and treatment. *Altern. Med. Rev.* **2006,** *11*, (1), 2-22.
5. Graziano, J. H.; Blum, C. B.; Lolacono, N. J.; Slavkovich, V.; Manton, W. I.; Pond, S.; Moore, M. R., Human in vivo model for the determination of lead bioavailability using stable isotope dilution. *Environ. Health Perspect.* **1996,** *104*, (2), 176-179.
6. van Elteren, J. T.; Grilc, M.; Beeston, M. P.; Reig, M. S.; Grgic, I., An integrated experimental-modeling approach to study the acid leaching behavior of lead from sub-micrometer lead silicate glass particles. *J. Hazard. Mater.* **2013,** *262*, 240-249.
7. Rahimi, R. A.; Sadrnezhaad, S. K., Effects of Ion-Exchange and Hydrolysis Mechanisms on Lead Silicate Glass Corrosion. *Corrosion* **2012,** *68*, (9), 793-800.
8. Rahimi, R. A.; Sadrnezhaad, S. K.; Raisali, G.; Hamidi, A., Hydrolysis kinetics of lead silicate glass in acid solution. *Journal of Nuclear Materials* **2009,** *389*, (3), 427-431.
9. Sadrnezhaad, S. K.; Rahimi, R. A.; Raisali, G.; Foruzanfar, F., Mechanism of deleading of silicate glass by 0.5 N HNO3. *Journal of Non-Crystalline Solids* **2009,** *355*, (48-49), 2400-2404.
10. Mizuno, M.; Takahashi, M.; Takaishi, T.; Yoko, T., Leaching of lead and connectivity of plumbate networks in lead silicate glasses. *J. Am. Ceram. Soc.* **2005,** *88*, (10), 2908-2912.
11. Bertoncello, R.; Milanese, L.; Bouquillon, A.; Dran, J. C.; Mille, B.; Salomon, J., Leaching of lead silicate glasses in acid environment: compositional and structural changes. *Appl. Phys. A-Mater. Sci. Process.* **2004,** *79*, (2), 193-198.
12. Bonnet, C.; Bouquillon, A.; Turrell, S.; Deram, V.; Mille, B.; Salomon, J.; Thomassin, J. H.; Fiaud, C., Alteration of lead silicate glasses due to leaching in heated acid solutions. *Journal of Non-Crystalline Solids* **2003,** *323*, (1-3), 214-220.
13. Guadagnino, E.; Gambaro, M.; Gramiccioni, L.; Denaro, M.; Feliciani, R.; Baldin, M.; Stacchini, P.; Giovannangeli, S.; Carelli, G.; Castellino, N.; Vinci, F., Estimation of lead intake from crystalware under conditions of consumer use. *Food Addit. Contam.* **2000,** *17*, (3), 205-218.
14. Guadagnino, E.; Verita, M.; Geotti-Bianchini, F.; Shallenberger, J.; Pantano, C. G., Surface analysis of 24% lead crystal glass articles: correlation with lead release. *Glass Technol.* **2002,** *43*, (2), 63-69.
15. Schultz-Munzenberg, C.; Meisel, W.; Gutlich, P., Changes of lead silicate glasses induced by leaching. *Journal of Non-Crystalline Solids* **1998,** *238*, (1-2), 83-90.

16. Ahmed, A. A.; Youssof, I. M., Effect of repeated leaching on the release of lead and other cations from lead crystal glass (24% PbO) by acid solutions and water. *Glass Technol.* **1997,** *38*, (5), 171-178.

17. Ahmed, A. A.; Youssof, I. M., Interaction between lead crystal glass (24 % PbO) and acetic acid. *Glastech. Ber.-Glass Sci. Technol.* **1997,** *70*, (6), 173-185.

18. Ahmed, A. A.; Youssof, I. M., Reactions between water and lead crystal glass (24% PbO). *Glass Technol.* **1997,** *38*, (1), 30-38.

19. Cailleteau, C.; Weigel, C.; Ledieu, A.; Barboux, P.; Devreux, F., On the effect of glass composition in the dissolution of glasses by water. *Journal of Non-Crystalline Solids* **2008,** *354*, (2-9), 117-123.

20. Graziano, J. H.; Blum, C., LEAD-EXPOSURE FROM LEAD CRYSTAL. *Lancet* **1991,** *337*, (8734), 141-142.

21. Kanunnikova, O. M.; Goncharov, O. Y., X-ray photoelectron analysis of lead-silicate glass structure. *J. Appl. Spectrosc.* **2009,** *76*, (2), 194-202.

22. Wang, P. W.; Zhang, L. P., Structural role of lead in lead silicate glasses derived from XPS spectra. *Journal of Non-Crystalline Solids* **1996,** *194*, (1-2), 129-134.

23. Alderman, O. L. G.; Hannon, A. C.; Holland, D.; Feller, S.; Lehr, G.; Vitale, A. J.; Hoppe, U.; von Zimmerman, M.; Watenphul, A., Lone-pair distribution and plumbite network formation in high lead silicate glass, 80PbO center dot 20SiO(2). *Phys. Chem. Chem. Phys.* **2013,** *15*, (22), 8506-8519.

24. Takaishi, T.; Takahashi, M.; Jin, J.; Uchino, T.; Yoko, T.; Takahashi, M., Structural study on PbO-SiO2 glasses by X-ray and neutron diffraction and Si-29 MAS NMR measurements. *J. Am. Ceram. Soc.* **2005,** *88*, (6), 1591-1596.

25. Gee, I. A.; Holland, D.; McConville, C. F., Atomic environments in binary lead silicate and ternary alkali lead silicate glasses. *Phys. Chem. Glasses* **2001,** *42*, (6), 339-348.

26. Fayon, F.; Landron, C.; Sakurai, K.; Bessada, C.; Massiot, D., Pb2+ environment in lead silicate glasses probed by Pb-L-III edge XAFS and Pb-207 NMR. *Journal of Non-Crystalline Solids* **1999,** *243*, (1), 39-44.

27. Feller, S.; Lodden, G.; Riley, A.; Edwards, T.; Croskrey, J.; Schue, A.; Liss, D.; Stentz, D.; Blair, S.; Kelley, M.; Smith, G.; Singleton, S.; Affatigato, M.; Holland, D.; Smith, M. E.; Kamitsos, E. I.; Varsamis, C. P. E.; Ioannou, E., A multispectroscopic structural study of lead silicate glasses over an extended range of compositions. *Journal of Non-Crystalline Solids* **2010,** *356*, (6-8), 304-313.

28. Fajans, K.; Kreidl, N. J., STABILITY OF LEAD GLASSES AND POLARIZATION OF IONS. *J. Am. Ceram. Soc.* **1948,** *31*, (4), 105-114.

29. Carmona, N.; Garcia-Heras, M.; Gil, C.; Villegas, M. A., Chemical degradation of glasses under simulated marine medium. *Mater. Chem. Phys.* **2005,** *94*, (1), 92-102.

30. Hight, S. C., Lead migration from lead crystal wine glasses. *Food Addit. Contam.* **1996,** *13*, (7), 747-765.

31. Angeli, F.; Charpentier, T.; Gaillard, M.; Jollivet, P., Influence of zirconium on the structure of pristine and leached soda-lime borosilicate glasses: Towards a quantitative approach by O-17 MQMAS NMR. *Journal of Non-Crystalline Solids* **2008,** *354*, (31), 3713-3722.

32. Larsen, F. H.; Farnan, I., Si-29 and O-17 (Q)CPMG-MAS solid-state NMR experiments as an optimum approach for half-integer nuclei having long T-1 relaxation times. *Chem. Phys. Lett.* **2002,** *357*, (5-6), 403-408.

33. Amoureux, J. P.; Fernandez, C.; Steuernagel, S., Z filtering in MQMAS NMR. *J. Magn. Reson. Ser. A* **1996,** *123*, (1), 116-118.

34. Fernandez, C.; Amoureux, J. P., 2D MULTIQUANTUM MAS-NMR SPECTROSCOPY OF AL-27 IN ALUMINOPHOSPHATE MOLECULAR-SIEVES. *Chem. Phys. Lett.* **1995,** *242*, (4-5), 449-454.

35. Angeli, F.; Villain, O.; Schuller, S.; Ispas, S.; Charpentier, T., Insight into sodium silicate glass structural organization by multinuclear NMR combined with first-principles calculations. *Geochim. Cosmochim. Acta* **2011,** *75*, (9), 2453-2469.

36. Fayon, F.; Bessada, C.; Massiot, D.; Farnan, I.; Coutures, J. P., Si-29 and Pb-207 NMR study of local order in lead silicate glasses. *Journal of Non-Crystalline Solids* **1998,** *232*, 403-408.

37. Shrikhande, V. K.; Sudarsan, V.; Kothiyal, G. P.; Kulshreshtha, S. K., Si-29 MAS NMR and microhardness studies of some lead silicate glasses with and without modifiers. *Journal of Non-Crystalline Solids* **2001,** *283*, (1-3), 18-26.

38. Lee, S. K.; Kim, E. J., Probing Metal-Bridging Oxygen and Configurational Disorder in Amorphous Lead Silicates: Insights from O-17 Solid-State Nuclear Magnetic Resonance. *Journal of Physical Chemistry C* **2015,** *119*, (1), 748-756.

39. Florian, P.; Vermillion, K. E.; Grandinetti, P. J.; Farnan, I.; Stebbins, J. F., Cation distribution in mixed alkali disilicate glasses. *J. Am. Chem. Soc.* **1996,** *118*, (14), 3493-3497.

40. Lee, S. K.; Stebbins, J. F., Effects of the degree of polymerization on the structure of sodium silicate and aluminosilicate glasses and melts: An O-17 NMR study. *Geochim. Cosmochim. Acta* **2009,** *73*, (4), 1109-1119.

41. Clark, T. M.; Grandinetti, P. J., Calculation of bridging oxygen O-17 quadrupolar coupling parameters in alkali silicates: A combined ab initio investigation. *Solid State Nucl. Magn. Reson.* **2005,** *27*, (4), 233-241.

42. Clark, T. M.; Grandinetti, P. J.; Florian, P.; Stebbins, J. F., An O-17 NMR investigation of crystalline sodium metasilicate: Implications for the determination of local structure in alkali silicates. *Journal of Physical Chemistry B* **2001,** *105*, (49), 12257-12265.

43. Ashbrook, S. E.; Berry, A. J.; Wimperis, S., O-17 multiple-quantum MAS NMR study of high-pressure hydrous magnesium silicates. *J. Am. Chem. Soc.* **2001,** *123*, (26), 6360-6366.

44. Ashbrook, S. E.; Berry, A. J.; Wimperis, S., O-17 multiple-quantum MAS NMR study of pyroxenes. *Journal of Physical Chemistry B* **2002,** *106*, (4), 773-778.

45. Lee, S. K.; Stebbins, J. F., Nature of cation mixing and ordering in Na-Ca silicate glasses and melts. *Journal of Physical Chemistry B* **2003,** *107*, (14), 3141-3148.

46. Angeli, F.; Charpentier, T.; Molieres, E.; Soleilhavoup, A.; Jollivet, P.; Gin, S., Influence of lanthanum on borosilicate glass structure: A multinuclear MAS and MQMAS NMR investigation. *Journal of Non-Crystalline Solids* **2013,** *376*, 189-198.

47. Gin, S.; Jollivet, P.; Fournier, M.; Angeli, F.; Frugier, P.; Charpentier, T., Origin and consequences of silicate glass passivation by surface layers. *Nature Communications* **2015,** *6*.

48. Helebrant, A.; Pekarkova, I., Kinetics of glass corrosion in acid solutions. *Ber. Bunsen-Ges. Phys. Chem. Chem. Phys.* **1996,** *100*, (9), 1519-1522.
49. Apelblat, A.; Manzurola, E., Solubilities of manganese, cadmium, mercury and lead acetates in water from T=278.15 K to T=340.15 K. *J. Chem. Thermodyn.* **2001,** *33*, (2), 147-153.
50. Fournier, M.; Ull, A.; Nicoleau, E.; Inagaki, Y.; Odorico, M.; Frugier, P.; Gin, S., Glass dissolution rate measurement and calculation revisited. *Journal of Nuclear Materials* **2016,** *476*, 140-154.
51. Brunet, F.; Charpentier, T.; Le Caer, S.; Renault, J. P., Solid-state NMR characterization of a controlled-pore glass and of the effects of electron irradiation. *Solid State Nucl. Magn. Reson.* **2008,** *33*, (1-2), 1-11.
52. Charpentier, T.; Kroll, P.; Mauri, F., First-Principles Nuclear Magnetic Resonance Structural Analysis of Vitreous Silica. *Journal of Physical Chemistry C* **2009,** *113*, (18), 7917-7929.

Table caption

	Site	^{17}O NMR Parameters		Proportion from composition	Proportion from ^{17}O NMR
Pristine glass	Si-O-Si	$C_Q(MHz)-(\sigma_{C_Q})$	52.5 (7.3) 4.8 (0.3)	78 %	78 %
		$\eta_Q-(\sigma_{\eta_Q})$	0.3 (0.1)		
	Si-O-(Pb,K)	$\delta_{iso}(ppm)-(\sigma_{\delta_{iso}})$	118.7 (10.8)	9 % (Si-O-Pb)	14 %
		$C_Q(MHz)-(\sigma_{C_Q})$	3.1 (0.5)		
		$\eta_Q-(\sigma_{\eta_Q})$	0.6 (0.2)		
	Si-O-K	$\delta_{iso}(ppm)-(\sigma_{\delta_{iso}})$	74.8 (9.2)	13 %	8 %
		$C_Q(MHz)-(\sigma_{C_Q})$	2.2 (0.5)		
		$\eta_Q-(\sigma_{\eta_Q})$	0.6 (0.2)		
Altered glass	Si-O-Si	$\delta_{iso}(ppm)-(\sigma_{\delta_{iso}})$	42.0 (5.0)	89 %	89 %
		$C_Q(MHz)-(\sigma_{C_Q})$	5.2 (0.2)		
		$\eta_Q-(\sigma_{\eta_Q})$	0.2 (0.1)		
	Si-O-(Pb,K)	$\delta_{iso}(ppm)-(\sigma_{\delta_{iso}})$	130.0 (12.0)	8 % (Si-O-Pb)	6 %
		$C_Q(MHz)-(\sigma_{C_Q})$	3.1 (0.5)		
		$\eta_Q-(\sigma_{\eta_Q})$	0.6 (0.2)		
	Si-O-K	$\delta_{iso}(ppm)-(\sigma_{\delta_{iso}})$	74.8 (9.2)	3 %	1 %
		$C_Q(MHz)-(\sigma_{C_Q})$	2.2 (0.5)		
		$\eta_Q-(\sigma_{\eta_Q})$	0.6 (0.2)		
	Si-O-H	$\delta_{iso}(ppm)-(\sigma_{\delta_{iso}})$	130.0 (12.0)	-	4 %
		$C_Q(MHz)-(\sigma_{C_Q})$	3.1 (0.5)		
		$\eta_Q-(\sigma_{\eta_Q})$	0.6 (0.2)		

Table 1. *^{17}O NMR parameters obtained by fitting the ^{17}O MAS NMR data of pristine and altered glass (standard deviations, depending on the distribution of each parameter, are indicated in parentheses) using as constraints the parameters extracted from the MQMAS data. The C_Q precision is 0.25 MHz and δ_{iso} precision is 2 ppm. The site proportions, calculated from pristine and altered glass compositions, and from the ^{17}O MAS NMR data, are reported.*

Figure caption

(a) *(b)*

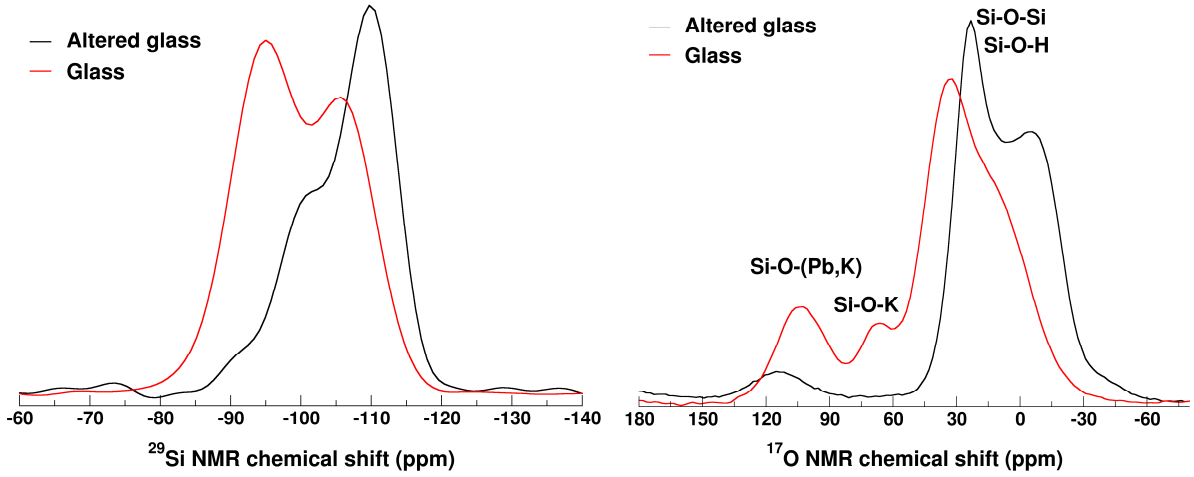

Figure 1. *(a) ^{29}Si MAS NMR and (b) ^{17}O MAS NMR spectra of pristine and altered glass after 35 days at 70℃ in acetic acid solution with oxygen-17 enri ched water.*

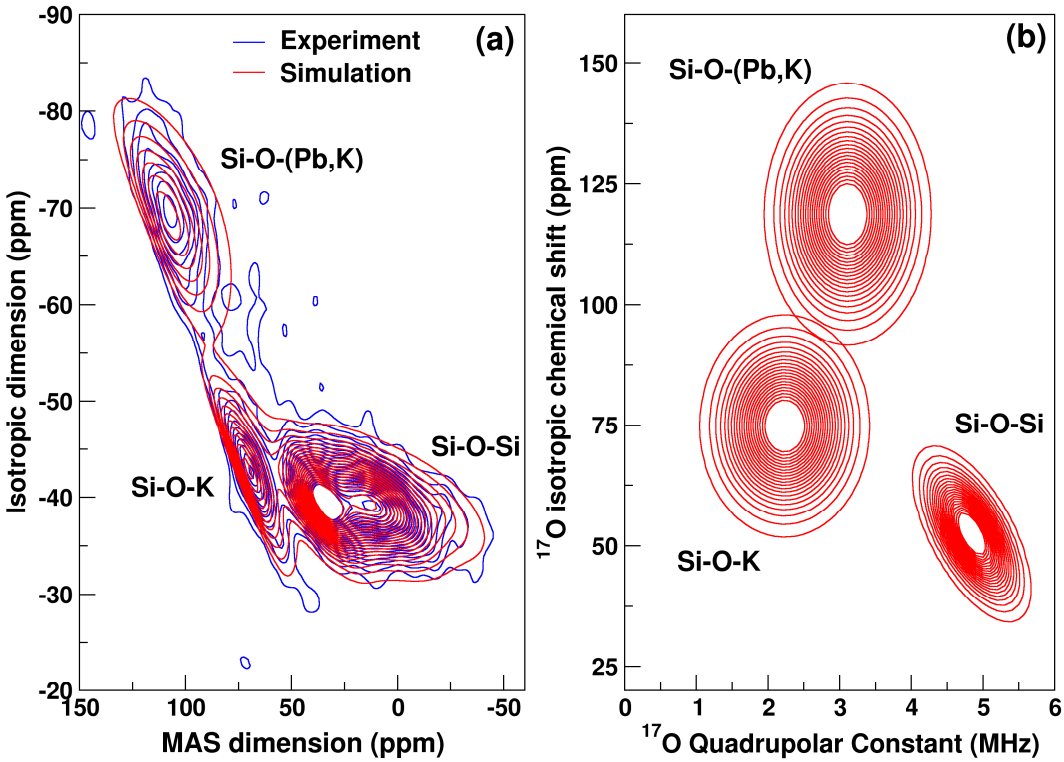

Figure 2. *(a) Contour plots of the experimental and simulated ^{17}O MQMAS spectra and (b) the two-dimensional projection of the extracted ^{17}O NMR parameter distributions δ_{iso} and C_Q.*

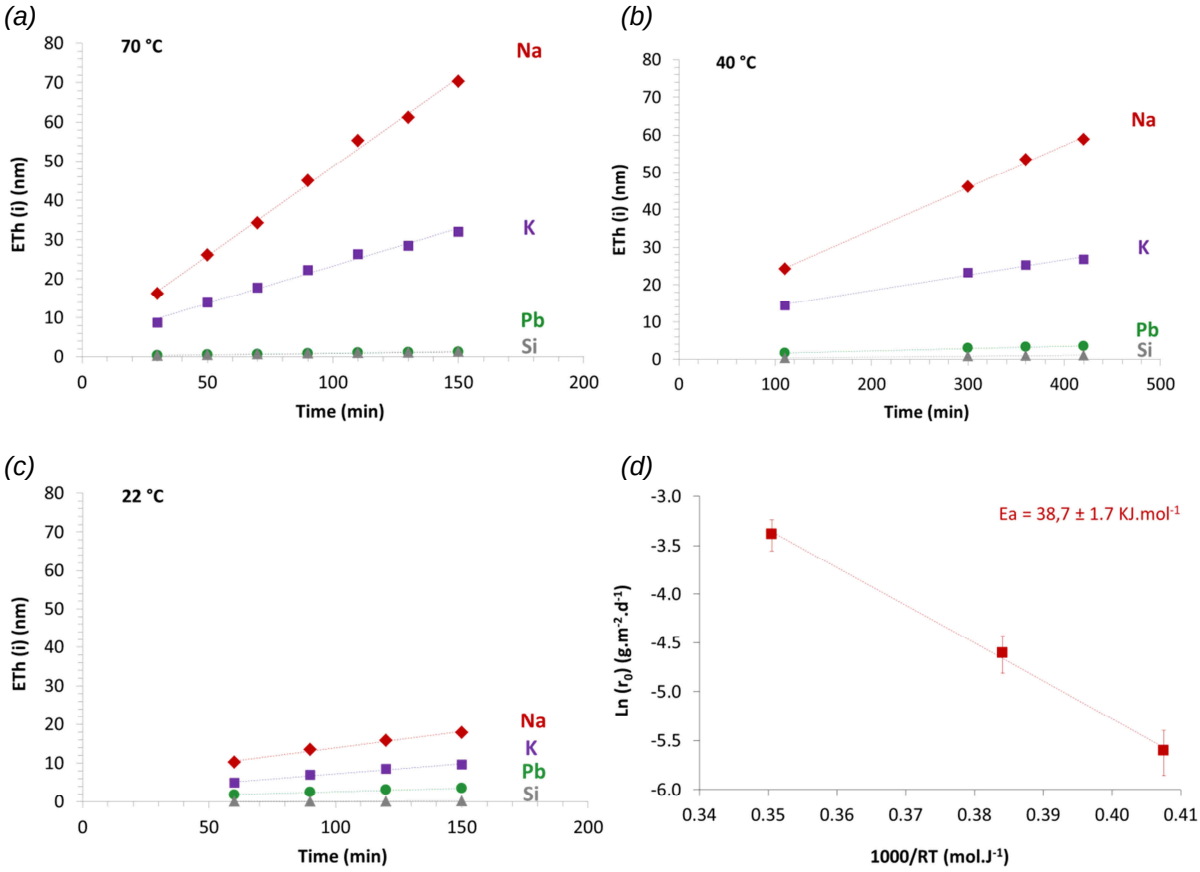

***Figure 3**. Equivalent thickness of altered glass calculated from the release of Si at 22℃ (a), 40℃ (b) and 70℃ (c) in acetic acid, in forward dissolution rate regime. (d) Determination of the apparent activation energy for the alteration mechanisms in forward dissolution rate regime. Broken lines are simple visual aids.*

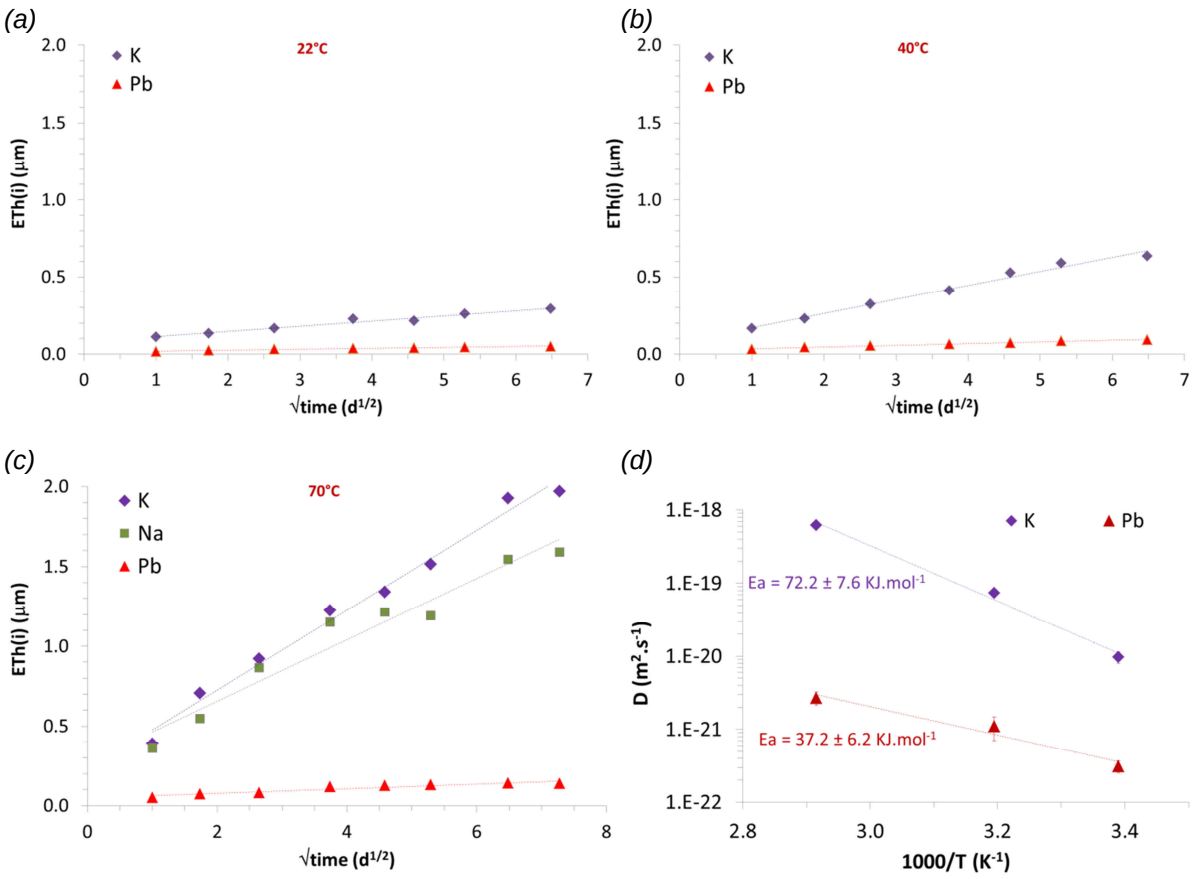

***Figure 4**. Equivalent thickness of altered glass calculated from the leaching of Pb and of K at 22℃ (a), 40℃ (b) and 70℃ (b) in acetic acid solution, in a solution initially saturated with respect to amorphous silica. (d) Representation of the diffusion coefficients depending on the temperature. The activation energy (Ea) is given by the slope of the line. Broken lines are simple visual aids.*

(a) *(b)*

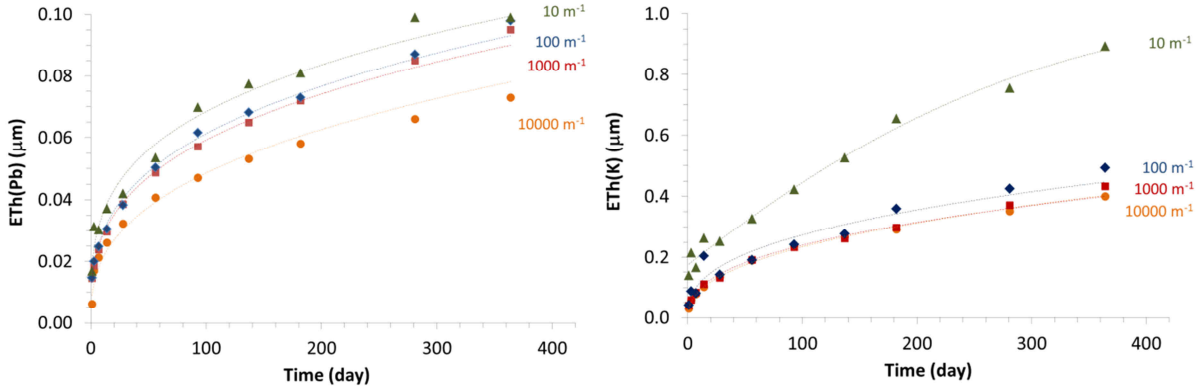

***Figure 5**. Equivalent thickness of altered glass calculated from the release of (a) Pb and (b) K at 22℃ in acetic acid solution for different SA/V ratios (10, 100, 1000 and 10000 m^{-1}). Broken lines are simple visual aids.*

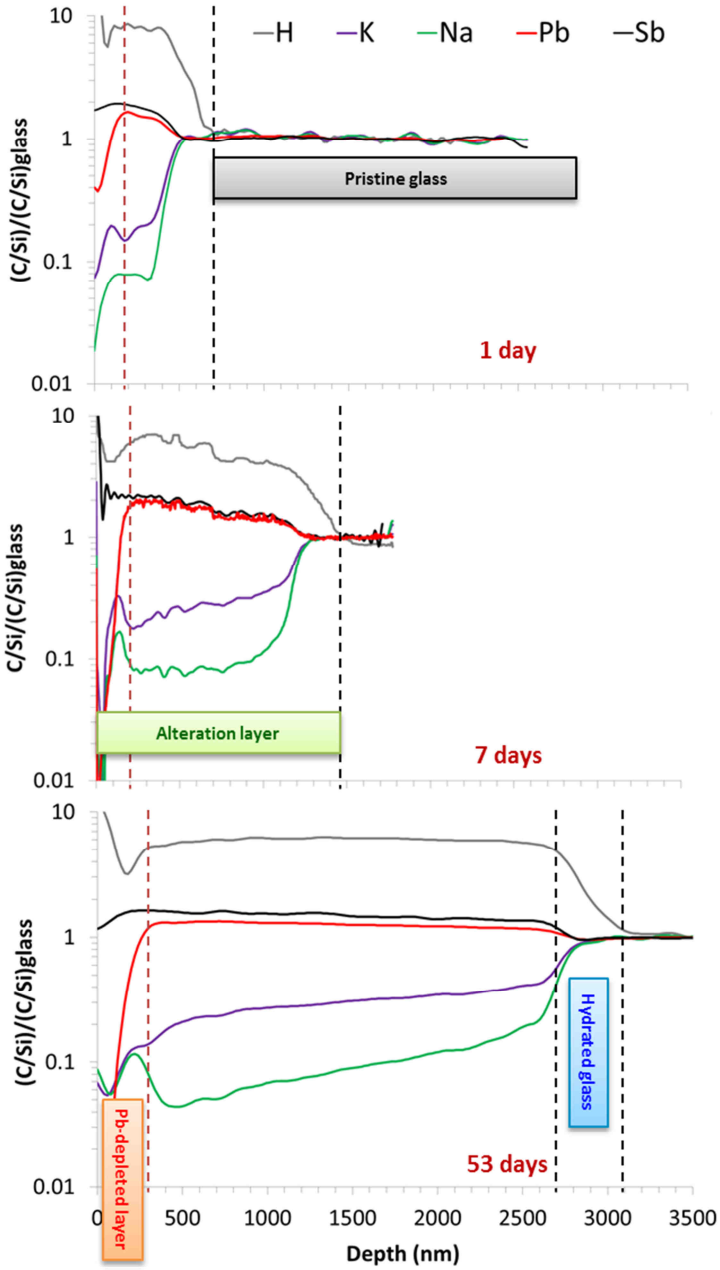

***Figure 6**. Elemental profiles obtained by ToF-SIMS on the glass altered at 70℃ for 1, 7 and 53 days in acetic acid solution saturated with respect to amorphous silica. Data have been normalized compared to Si, which is the least soluble element. All the elements are thus normalized to 1 in the pristine glass; data lower than 1 indicate a depletion of the element, whereas data higher than 1 indicate an enrichment*

Supplementary information

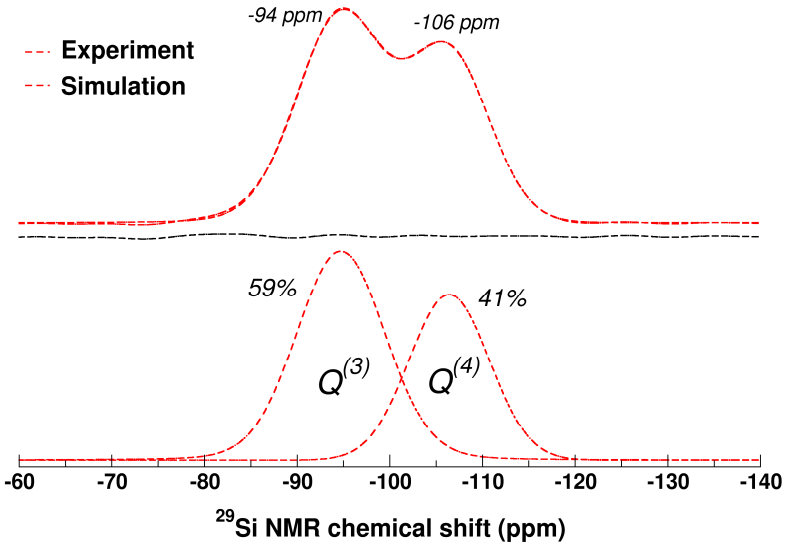

Figure S1. *^{29}Si MAS NMR spectra of pristine glass (solid line) and simulated spectra (dotted lines)*

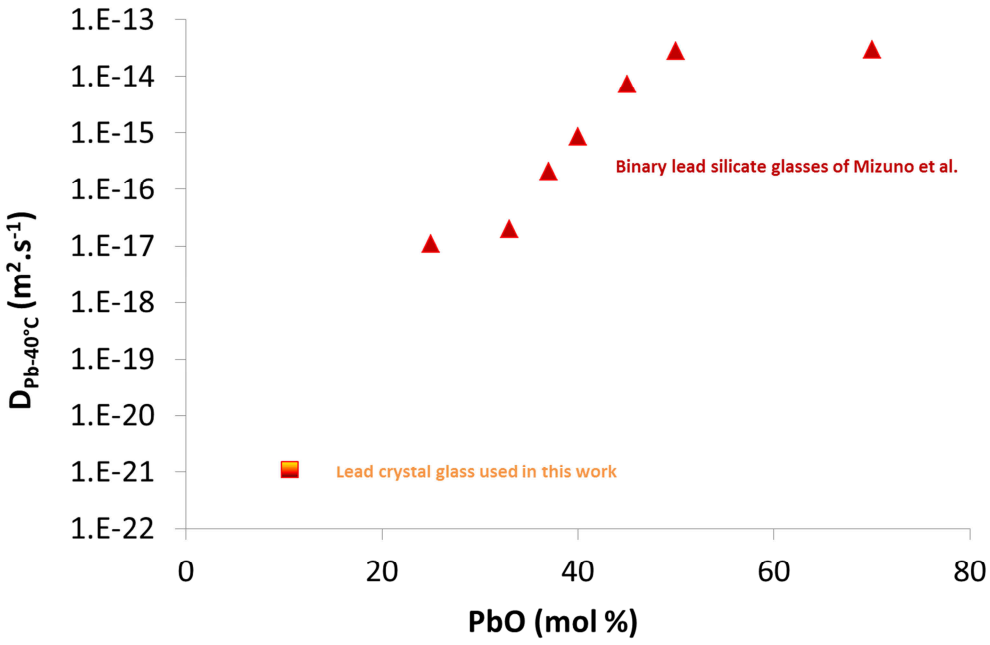

Figure S2. *Comparison of diffusion coefficients measured at 40℃ in the lead crystal glass used in this work and in binary lead silicate glasses of Mizuno et al. [10].*

(a)

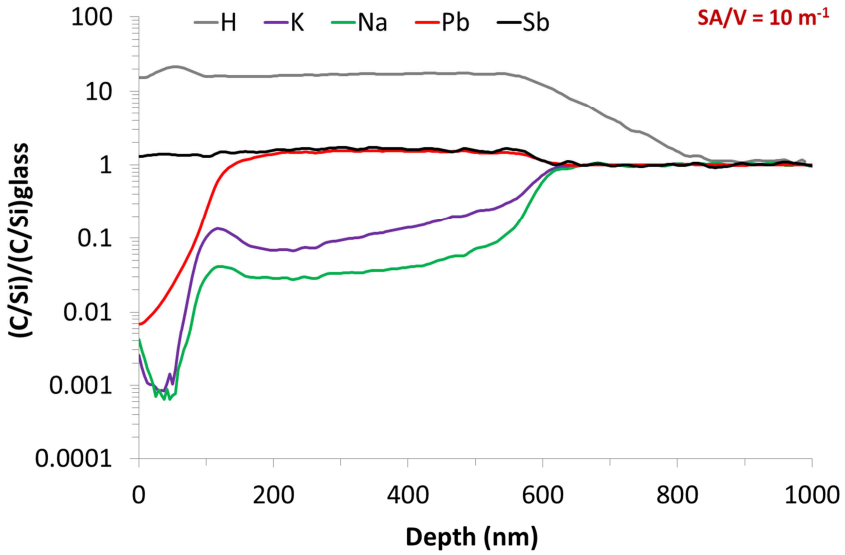

(b)

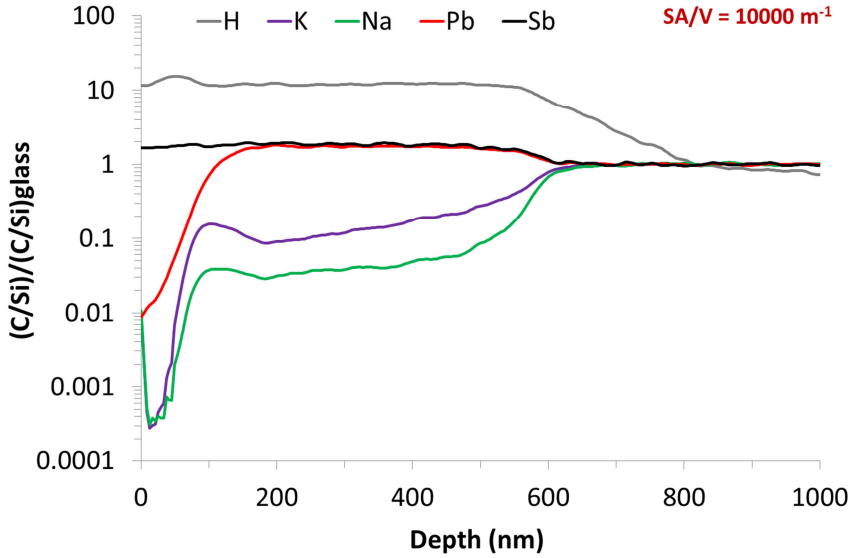

Figure S3. *Elemental profiles obtained by ToF-SIMS on the glass altered at 22℃ for 1 year in acetic acid solution with SA/V = 10 m^{-1} (a) and SA/V = 10000 m^{-1} (b). Data have been normalized compared to Si, which is the least soluble element. All the elements are thus normalized to 1 in the pristine glass; data lower than 1 indicate a depletion of the element, whereas data higher than 1 indicate an enrichment.*

(a) (b)

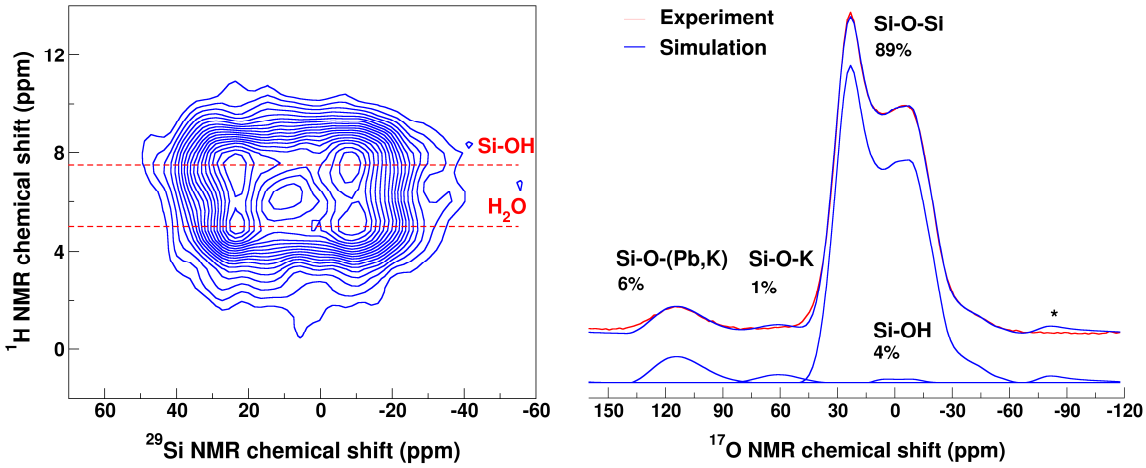

Figure S4. *(a) $^{1}H \rightarrow {}^{17}O$ HETCOR spectra with 2 ms polarization time of altered glass. (b) Simulation of the ^{17}O MAS NMR spectra of altered glass (35 days at 70℃ in acetic acid solution with oxyge n-17 enriched water).*

For Table of Contents Only